European Journal of Drug Metabolism and Pharmacokinetics (2020) 45:523–533
https://doi.org/10.1007/s13318-020-00618-4

ORIGINAL RESEARCH ARTICLE

UFLC–MS/MS Determination and Population Pharmacokinetic Study of Tanshinol, Ginsenoside Rb1 and Rg1 in Rat Plasma After Oral Administration of Compound Danshen Dripping Pills

Tianqian Jin[1,2,3] · Zuhui Liu[1,2,3] · Yang Chu[1,2] · Xiaohui Ma[1,2] · Shuming Li[1,2] · Xiangyang Wang[1,2] · Genbei Wang[1,2] · Shuiping Zhou[1,2] · He Sun[1,2,4] · Jin Yang[3]

Published online: 17 April 2020

Abstract

Background and Objectives As a traditional Chinese Materia Medica (CMM), the Compound Danshen Dripping Pill (CDDP) is widely used for the treatments of cardiovascular diseases. In view of its undefined applicable population and dosage, a population pharmacokinetic (PPK) study is required. The objective of this study was to explore the feasibility of multi-component CMM PPK in rat plasma after oral administration of CDDP based on sparse sampling.

Methods In this research, a simple, rapid and highly sensitive UFLC–MS/MS method for the simultaneous determination of tanshinol (TSL), ginsenoside Rb1 (GRb1) and ginsenoside Rg1 (GRg1) has been successfully developed in rat plasma. Moreover, the validated method has been applied to a PPK study of CDDP based on sparse data. We established the PPK models for these three main active constituents using a nonlinear mixed-effects model, taking into account of factors such as gender, age in weeks and weight.

Results The PPK models of TSL and GRb1 were best described by a one-compartment model with linear elimination and first-order absorption. The model of GRg1 was best described by a two-compartment model with first-order absorption. Bootstrap validation and a visual predictive check confirmed the predictive ability, the model stability and the precision of the parameter estimates from these models.

Conclusion As a preliminary exploration toward the clinical population pharmacokinetic research, this study provides a reference for the population pharmacokinetic study of traditional CMM.

Key Points

A UFLC-MS/MS method for the simultaneous determination of tanshinol (TSL), ginsenoside Rb1 (GRb1) and ginsenoside Rg1 (GRg1) has been established.

Sparse sampling can provide a reference for clinical PPK research.

PPK models using the a nonlinear mixed-effects method for compound Chinese medicine has been established.

Tianqian Jin, Zuhui Liu and Yang Chu contributed equally to this work.

✉ Jin Yang
yjcpu@yahoo.com

1 Tasly Academy, Tasly Holding Group Co., Ltd., Tianjin 300410, China

2 State Key Laboratory of Critical Technology in Innovative Chinese Medicine, Tasly Pharmaceutical Group Co., Ltd., Tianjin 300410, China

3 Center of Drug Metabolism and Pharmacokinetics, China Pharmaceutical University, Nanjing 210009, China

4 Tasly Pharmaceuticals Inc, Rockville, MD 20850, USA

1 Introduction

The Compound Danshen Dripping Pill (CDDP) is a modern Chinese medicine compound, which was recorded by the Chinese Pharmacopeia in 1990. It has been widely used for the prevention and treatment of cardiovascular diseases, including angina pectoris, coronary arteriosclerosis [1]. Several studies have demonstrated the pharmacologic effects and action mechanism of CDDP: inhibition of platelet adhesion and aggregation, anti-oxidative and anti-inflammatory, modulate energy metabolism, improvement of microcirculation, etc. [2–4]. These cardioprotective functions of CDDP are attributed to the various active substances including phenolic acids from *Radix salviae miltiorrhizae* [5, 6] and saponins from *R. notoginseng* [7, 8], such as tanshinol (TSL) [9, 10], protocatechuic aldehyde (PCA) [11], salvianolic acids, ginsenoside Rb1 (GRb1) [12–14], and ginsenoside Rg1 (GRg1) [15, 16], and notoginsenoside R1 (NR1).

With the development of analysis methods, the chemical basis of CDDP has been extensively studied in animals and humans. Lu et al. [17] indicated that TSL from *R. salviae miltiorrhizae* is a promising pharmacokinetic marker for CDDP, while other active phenolic acids show poor gut permeability or low plasma levels. Li et al. [18] reported NR1, GRg1 and GRb1 as pharmacokinetic markers of *R. notoginseng*. The existing pharmacokinetic studies [19–21] on these major active ingredients have provided a basis for elucidating the efficacy of CDDP, but research and application processes still face some problems. Firstly, compositions of CDDP are complex, and the pharmacokinetic characteristics are quite different. Several animal studies [18, 22] have reported that the half-life ($T_{1/2\beta}$) of GRb1 was obviously longer than those of GRg1 and TSL. In studying the whole pharmacokinetic process of CDDP, we have to face a longtime span of pharmacokinetic research and dense sampling (5, 15, 30 and 45 min and 1, 1.5, 2, 3, 4, 6, 8, 10, 12, 24, 48 and 72 h after dosing). In non-clinical studies, the amount of blood collected is relatively large, which cannot perfectly conform to animal experiment specifications with traditional sampling methods. Secondly, similar to the concept of individualized drug administration, the clinical application of traditional Chinese Materia Medica (CMM) pays attention to "dialectical treatment". However, traditional Chinese medicine treatment based on syndrome differentiation often relies on the experience of doctors, and there are some uncertainties. At this point, research on the precise medication and dosage adjustment for CDDP has not been carried out.

It is well known that by combining classical pharmacokinetic principles with statistical models (i.e. a nonlinear mixed-effects model), population pharmacokinetics (PPK) can effectively utilize sparse data for pharmacokinetic analysis. It also provides a quantitative estimation of the inter/intra-subject variability in pharmacokinetic response and the influence of demographic, clinical and genetic factors on the dose–concentration relationship [23]. Applied to multi-factor integrated individualized treatment, PPK is very consistent with the essence of traditional Chinese medicine philosophy. By searching the existing literature, sparse sampling has been used to describe multi-component PPK studies. In this study, we first attempted to establish PPK models for TSL, GRb1 and GRg1 in rat plasma after oral CDDP based on sparse data. We also quantitatively evaluated the effects of demographic characteristics including gender, week age, and body weight on pharmacokinetic parameters. With the help of advanced model tools, we explored the feasibility of multi-component CMM PPK research based on sparse sampling, and hope to provide a reference for a clinical PPK study of traditional Chinese medicine.

2 Material and Methods

2.1 Determination of Plasma Concentration of CDDP Constituents

2.1.1 Chemicals and Reagents

The standards of TSL, GRb1, GRg1, chloramphenicol (internal standard for TSL, IS-1) and estazolam (internal standard for GRb1 and GRg1, IS-2) were purchased from the Chinese National Institute for the Control of Pharmaceutical and Biological Products (Beijing, China). CDDP (batch number: 170,203; the content of the tanshinol in each pill is about 0.27 mg, ginsenoside Rb1 is about 0.12 mg, ginsenoside Rg1 is about 0.16 mg; Chinese Pharmacopoeia stipulates that each pill contains Danshen based on tanshinol, which should not be less than 0.10 mg since tanshinol is considered as the main effective compound) was supplied by the Tasly Pharmaceutical Group (Tianjin, China). Acetonitrile and methanol (Merck, Germany) and formic acid (Fisher Scientific, USA) were of HPLC-grade. The water (> 18.2 mΩ) was purified by a Milli-Q water purification system (Milford, MA, USA). All the other analytical grade reagents, such as *N*-butanol, ethyl acetate, hydrochloric acid and sodium bisulfite, were purchased from commercial sources and were used without further purification.

2.1.2 Instrument and LC–MS/MS Conditions

Chromatographic separation was carried out on the Shimadzu UFLC system using an ACQUITY UPLC® HSS T3 column (1.8 µm, 2.1 mm × 100 mm) preceded by a VanGuard™ HSS T3 pre-column (1.8 µm, 2.1 mm × 5 mm) at 40 °C. A gradient mixture of 0.1% formic acid aqueous

Table 1 Mass spectrometry detection parameters (synchronization of positive and negative ion modes)

Parameters	Negative ion mode	Positive ion mode
Ion spray voltage	−4500 V	5500 V
Source temperature	450 °C	550 °C
Auxiliary gas (GS1, N_2)	45 psi	55 psi
Nebulizer gas (GS2, N_2)	45 psi	55 psi
Curtain gas (N_2)	20 psi	20 psi

solution (A) and acetonitrile (B) was constantly applied at a flow rate of 0.4 mL/min. The gradient elution program was: 5% B at 0–0.8 min, 5–90% B at 0.8–3.1 min, 90–5% B at 3.1–3.3 min, and 5% B at 3.3–4.5 min. The injection volume was 2 µL.

Samples were analyzed on a QTRAP® 5500 triple quadruple mass spectrometer (AB Sciex, Foster, CA, USA) with a Turbo V™ source interface. The positive ion mode and the negative ion mode were performed simultaneously. Instrument parameters were set to default values and each analyte was acquired in the optimized multiple reaction monitoring (MRM) mode. Relevant mass spectrometric conditions are listed in Table 1. The optimized MRM parameters of each compounds are listed in Table 2.

2.1.3 Standards and Quality Controls

TSL was dissolved in 0.1 M HCL (containing 0.2% sodium bisulfite) to form stock solutions of 1.0 mg/mL. GRb1 and GRg1 were dissolved in methanol to form a stock solution of 1.0 mg/mL, respectively. Three analytes were diluted to obtain the following mixture working solutions of 1.6, 3.2, 8, 24, 80, 240, 800, and 1600 ng TSL/mL methanol–water (1:1, v/v), of 0.5, 1, 2.5, 7.5, 25, 75, 250, and 500 ng GRb1/mL methanol–water (1:1, v/v) and of 0.1, 0.2, 0.5, 1.5, 5, 15, 50, and 100 ng GRg1/mL methanol–water (1:1, v/v). The mixed IS solutions were prepared at a concentration of 20 ng/mL methanol–water (1:1, v/v) for use. The standard curve samples were obtained by mixing plasma and the working solution in the same proportions after sample preparation, resulting in concentrations of 1.6–1600 ng/mL for TSL, 0.5–500 ng/mL for GRb1 and 0.1–100 ng/mL for GRg1. Quality control (QC) samples were prepared in the same process at low, medium and high concentrations: 4, 400, and 1200 ng/mL for TSL; 1.25, 125, and 375 ng/mL for GRb1; and 0.25, 25, and 75 ng/mL for GRg1.

2.1.4 Sample Preparation

An aliquot (100 µL) of rat plasma was mixed with 50 µL of mixed IS solution, 100 µL of methanol–water (1:1, v/v) and 100 µL of 1 M HCl. After vortexing for 3 min with 2 mL *N*-butanol-ethyl acetate (1:4, v/v), the sample was centrifuged (4500 rpm for 10 min) to obtain the supernatant, which was evaporated under nitrogen at 25 °C and resolved with 100 µL of acetonitrile–water (1:1, v/v). After the second centrifugation (13,000 rpm for 6 min), 2 µL of the supernatant was injected for analysis.

2.1.5 Method Validation

The established method was validated according to the FDA guidance for bioanalytical method validation. Chromatograms of blank plasma from six rats, corresponding plasma with the three compounds and ISs, and plasma samples after oral CDDP were compared to confirm that the assay was free of potential interfering substances.

The calibration curves were established by plotting the analyte/IS peak area ratios (y) versus the corresponding concentrations (x). The standard curve equation ($y = a + bx$) and correlation coefficient (r) were calculated using the weighted least square method ($1/x^2$). Six parallel QC samples were evaluated on the same day (intra-day) and on three different days (inter-day) to assess the precision and accuracy of the method. The precision was measured by the RSD and accuracy was evaluated by deviation between measured value and predetermined value (RSD < 15%, |RE| < 15%). The lower limit of quantitation (LLOQ) was defined as the lowest concentration of the standard curve that can be quantified with acceptable precision and accuracy (RSD < 20%, |RE| < 20%).

Table 2 The main mass parameters of TSL, IS-1, GRb1, GRg1 and IS-2

Analytes	Q1 (m/z)	Q3 (m/z)	DP (V)	EP(V)	CE(V)	CXP (V)	Polarity
TSL	197.3	134.8	−51	−10	−25	−16	Negative
IS-1	321.3	152.4	−65	−10	−24	−12	Negative
GRb1	1131.5	364.9	40	10	74	15	Positive
GRg1	823.6	643.5	59	10	51	12	Positive
IS-2	295.1	267.1	120	10	47	23	Positive

TSL tanshinol, *IS-1* internal standard for TSL, *GRb1* ginsenoside Rb1, *GRg1* ginsenoside Rg1, *IS-2* internal standard for GRb1 and GRg1, *Q1* precursor ion, *Q3* product ion, *DP* declustering potential, *EP* entrance potential, *CE* collision energy, *CXP* collision cell exit potential

Suppose A is the sample obtained by replacing plasma with equal amount of water during the preparation of the QC sample and B is the blank sample resolved with standard solution. The matrix effects (ME) at three QC levels were evaluated by comparing the responses of A with the QC samples and extraction recoveries were calculated by comparing the peak areas of B with the QC samples. The RSD of the IS-normalized MEs calculated from the six lots of the matrix should be less than 15%.

The stability of the analytes was guaranteed by analyzing six parallel samples at low and high QC levels under four conditions: exposure at 25 °C for 6 h, in an autosampler at 4 °C for 24 h, at − 40 °C for 2 weeks ,and three freeze–thaw cycles.

2.2 Population Pharmacokinetic Study of CDDP Constituents

2.2.1 Animal Experiments

All the rat experiments were approved by the Animal Ethics Committee of Tianjin Tasly Academy and conducted following the Guidelines for the Care and Use of Laboratory Animals. A total of 136 Wistar rats (50% male and 50% female) were included in the study. Male rats were 12.9 ± 4.3 (range 6–20) weeks old and weighed 375.8 ± 110.3 (range 163.3–603.0) g. Female rats were 13.1 ± 4.5 (range 6–21) weeks old and weighed 242.8 ± 57.2 (range 155.3–376.5) g. They were all obtained from Vital River Laboratory Animal Technology (Beijing, China). After 12 h fasting, the animals were given intragastric administration of dripping pills at a dosage of 1500 mg/kg with a syringe with a ball-tipped needle. The dosing solutions were prepared by dissolving CDDPs in normal saline to 0.3 g/mL in a plastic container. A series of blood samples of 500 μL (3–4 samples per animal) were collected from the jugular vein of each animal at times of 5, 15, 30 and 45 min and 1 h, 1.5, 2, 3, 4, 6, 8, 10, 12, 24, 48 and 72 h after dosing. The samples were centrifuged at 4500 rpm for 10 min to obtain plasma, which was stored at − 40 °C until analysis.

2.2.2 Population Pharmacokinetic Model Development

PPK models for TSL, GRb1 and GRg1 were developed with Phoenix NLME (v.8.0; Pharsight, USA) using the extended least square method (FOCE ELS). Based on Akaike's information criteria (AIC) value and coefficient of variation (CV%) of estimates, different compartment models with extravascular input were investigated to obtain the optimal structural model. The basic pharmacokinetic parameters estimated were the first-order absorption rate constant (K_a), volume of distribution (V/F) and oral clearance (CL/F).

The inter-individual variability was described with exponential models: $P_{ij} = \mathrm{tv}P_{ij} \times \exp(\eta_{ij})$, where P_j represents the jth pharmacokinetic parameter, I represents individual, tv represents the population typical value, and η_{ij} is a Gaussian random variable distributed with mean 0 and a variance of ω^2.

The residual error was described by the additive error model: Cobs = C + CEps, or the multiplicative error model: Cobs = $C \times (1 + \mathrm{CEps})$, where $C$is the predicted concentration, Cobs is the observed concentration. CEps is the default epsilon variable name, and represents a normal error with mean 0 and standard deviation σ.

After the basic model was selected, the Cov. Srch. Stepwise run mode was performed to screen the significant covariate based on the specified criterion options: add P value (0.01) and remove P value (0.001). Continuous covariates such as rat age (week) and body weight (WT) were introduced as a power model: $\mathrm{tv}P_{ij} = \mathrm{tv}P_j \times (\mathrm{week}_I/14)$ ^ $\mathrm{dP_j dweek} \times (\mathrm{WT_I}/260)$ ^ $\mathrm{dP_j dWT}$, where $\mathrm{dP_j dweek}$ and $\mathrm{dP_j dWT}$ are the corresponding fixed effect parameters. In addition, a categorical covariate as rat gender was introduced as follows: $\mathrm{tv}P_{ij} = \mathrm{tv}P_j \times \exp(\mathrm{dP_j dsex0} \times (\mathrm{sex} = 0))$, where (sex = 0) is a logical judgment symbol which returns 1 when the rat was female and 0 otherwise. To facilitate subsequent descriptions, for example, we use WT-K_a to refer to the effect of body weight on K_a.

We also used graphical methods and goodness-of-fit plots to evaluate the fitness of the final models, including observed concentrations (DV) versus individual predicted concentrations (IPRED) and population predicted concentrations (PRED), conditional weighted residuals (CWRES) versus time after dose (TAD) and PRED. Moreover, the accuracy, robustness and predictability of the final models were assessed by bootstrap validation and visual predictive check (VPC) based on 1000 re-samples.

3 Results

3.1 Method Development and Validation

A total of 136 (68 male and 68 female) Wistar rats were enrolled in the PPK research. The described UFLC–MS/MS method enables the simultaneous quantification of three compounds in CDDP.

Retention times observed were 2.39, 2.68 and 2.97 min for TSL, GRb1 and GRg1, respectively. And their typical chromatograms of blank plasma, plasma with the three compounds and ISs, and plasma samples after oral CDDP are shown in Fig. 1.

Tables 3 and 4 show the results of linearity, LLOQ, precision and accuracy obtained in the validation of the analytical methods. The assay was found to be linear referring

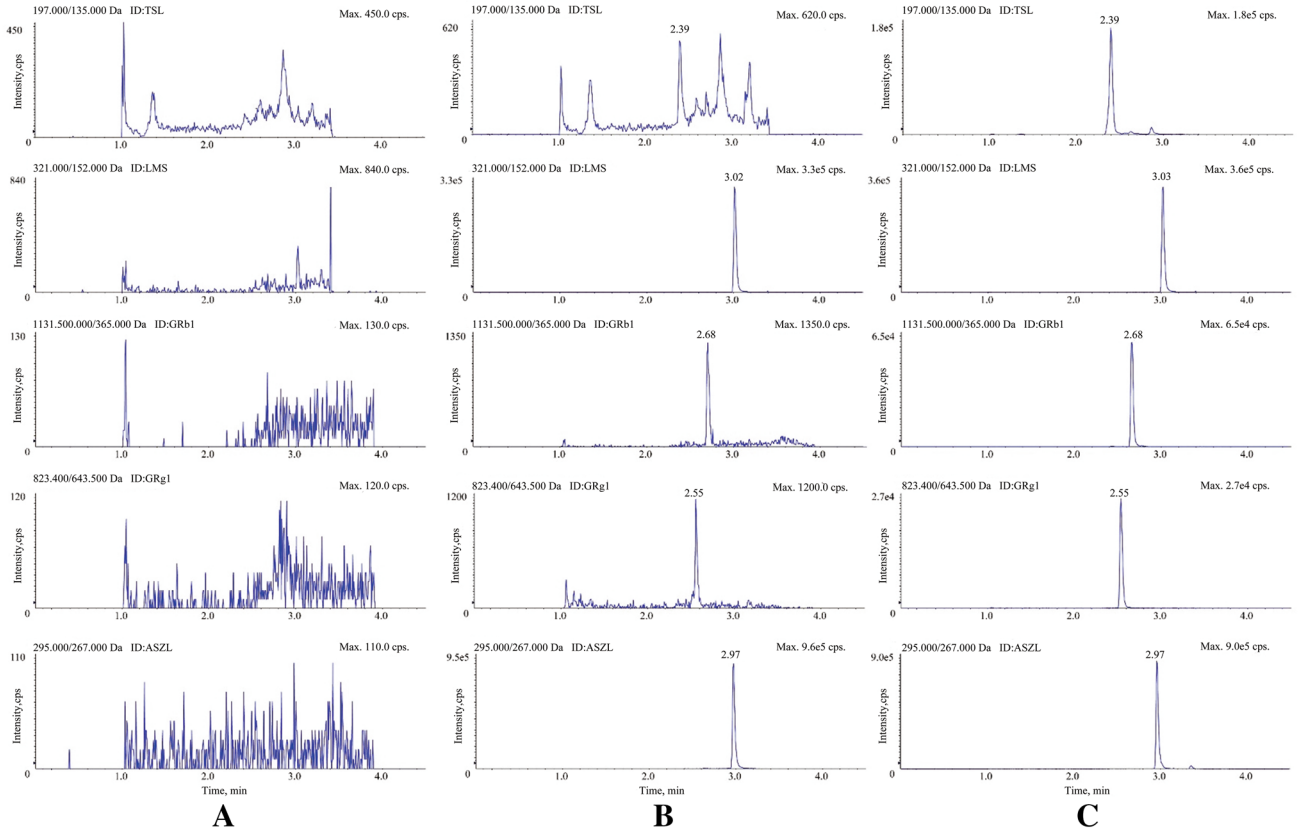

Fig. 1 Typical MRM chromatograms for analytes in rat plasma. From *top* to *bottom*, the *graphs* in each *row* are used to show the content of tanshinol, chloramphenicol (internal standard for tanshinol), ginsenoside Rb1, ginsenoside Rg1 and estazolam (internal standard for GRb1 and GRg1) separately. *Columns:* **a** only blank plasma; **b** plasma sample spiked with mixed standards; **c** plasma samples from a rat after oral CDDP. *TSL* tanshinol, *LMS* chloramphenicol, *GRb1* ginsenoside Rb1, *GRg1* ginsenoside Rg1, *ASZL* estazolam

Table 3 The linear ranges, regression equations and LLOQs of TSL, GRb1 and GRg1

Analytes	Regression equation	Linear range (ng/mL)	*r*	LLOQ (ng/mL)
TSL	$y = 0.00324x + 0.0094$	1.6–1600	0.9972	1.6
GRb1	$y = 0.00511x + 0.00088$	0.5–500	0.9924	0.5
GRg1	$y = 0.00722x + 0.0000748$	0.1–100	0.9965	0.1

r the correlation between the predicted values and the observed values, *LLOQ* the lower limit of quantitation

to the linear regression for the three compounds: TSL between 1.6 and 1600 ng/mL (slope: 0.00324, intercept: 0.00940, $r = 0.9972$); GRb1 between 0.5 and 500 ng/mL (slope: 0.00511, intercept: 0.00088, $r = 0.9924$); and GRg1 between 0.1 and 100 ng/mL (slope: 0.00722, intercept: 0.00007, $r = 0.9965$). The LLOQ were tested 1.6 ng/mL for TSL, 0.5 ng/mL for GRb1 and 0.1 ng/mL for GRg1. Intra- and inter-assay results showed that the methods had good reproducibility (RSD < 11.85%) and excellent accuracy ($-8.64\% < \text{RE} < 8.12\%$).

The matrix effects and recoveries of TSL, GRb1 and GRg1 were studied (Table 5). The matrix effects RSD values were between 4.09 and 11.01% (Table 5), which revealed the absence of endogenous substance interference. The method could offer good extraction efficiency, considering that the recovery values were over the range of 71.24–87.41% for TSL, 79.44–91.43% for GRb1 and 85.97–94.70% for GRg1. The stability test showed that the components were stable in rat plasma and processed samples under different conditions.

3.2 Population Pharmacokinetic Model

The objective function value (OFV) is − 2 times the log likelihood (LL) and AIC. Generally, the model with lower OFV

Table 4 The intra- and inter-day precision and accuracy of the three analytes

Analytes	Conc. (ng/mL)	Intra-day			Inter-day		
		Measured	RSD (%)	RE (%)	Measured	RSD (%)	RE (%)
TSL	1.6	1.67 ± 0.18	10.62	4.12	1.55 ± 0.18	11.85	− 3.04
	4	4.24 ± 0.36	8.48	6.00	3.99 ± 0.34	8.43	− 0.23
	400	426.09 ± 25.17	5.91	6.52	428.45 ± 19.23	4.49	7.11
	1200	1264.46 ± 58.14	4.59	5.37	1272.23 ± 65.65	5.16	6.02
GRb1	0.5	0.54 ± 0.03	5.86	8.12	0.54 ± 0.04	7.58	7.08
	1.25	1.26 ± 0.14	10.77	1.12	1.26 ± 0.11	8.94	0.43
	125	124.60 ± 7.96	6.39	− 0.32	121.53 ± 8.81	7.25	− 2.77
	375	354.23 ± 30.59	8.64	− 5.54	353.23 ± 23.69	6.71	− 5.81
GRg1	0.1	0.10 ± 0.01	9.32	− 1.60	0.10 ± 0.01	10.55	− 0.13
	0.25	0.26 ± 0.01	5.51	5.44	0.26 ± 0.02	6.15	3.84
	25	22.84 ± 1.12	4.91	− 8.64	24.37 ± 2.30	9.43	− 2.51
	75	75.58 ± 6.50	8.60	0.77	74.07 ± 6.56	8.85	− 1.24

RSD relative standard deviation, *RE* relative error

Table 5 Matrix effects and recoveries of the three analytes

Analytes	Conc. (ng/mL)	Matrix effect (%)	RSD (%)	Recovery (%)	RSD (%)
TSL	4	105.51 ± 7.24	6.87	78.95 ± 7.71	9.77
	400	107.44 ± 4.39	4.09	82.88 ± 4.53	5.47
	1200	108.35 ± 7.73	7.14	81.61 ± 4.56	5.59
GRb1	1.25	111.49 ± 11.73	10.53	87.89 ± 3.54	4.01
	125	116.34 ± 10.38	8.92	83.75 ± 3.04	3.62
	375	119.77 ± 7.76	6.48	84.62 ± 5.18	6.12
GRg1	0.25	103.75 ± 5.33	5.14	89.84 ± 2.86	3.19
	25	109.06 ± 12.01	11.01	88.97 ± 3.00	3.37
	75	98.67 ± 10.06	10.20	91.29 ± 3.41	3.74

Table 6 Screening of basic pharmacokinetic models of TSL

Basic pharmacokinetic models of TSL	OFV	AIC	If chosen (Y or N)
One-compartment model + additive error	3640.6	3654.6	N
One-compartment model + multiplicative error	3582.7	3596.7	Y
Two-compartment model + additive error	3628.0	3650.0	N
Two-compartment model + multiplicative error	3501.1	3523.1	N

Table 7 Screening of basic pharmacokinetic models of GRb1

Basic pharmacokinetic models of GRb1	OFV	AIC	If chosen (Y or N)
One-compartment model + additive error	3696.3	3710.3	N
One-compartment model + multiplicative error	3598.5	3610.6	Y
Two-compartment model + additive error	3695.2	3717.2	N
Two-compartment model + multiplicative error	3593.8	3615.8	N

Table 8 Screening of basic pharmacokinetic models of GRg1

Basic pharmacokinetic models of GRg1	OFV	AIC	If chosen (Y or N)
One-compartment model + additive error	950.0	964.0	N
One-compartment model + multiplicative error	914.1	928.1	N
Two-compartment model + additive error	859.7	881.7	Y
Two-compartment model + multiplicative error	804.5	826.5	N
Peripheral elimination model + additive error	2350.3	2372.3	N

and AIC values is considered better. Basic pharmacokinetic models of TSL (Table 6) and GRb1 (Table 7), including multiplicative errors, have lower OFV and AIC comparing to the model with additive error. The two-compartment model of GRb1 (Table 8) has lower OFV and AIC compared to the one-compartment model.

The plasma concentration–time profiles of TSL、GRb1 and GRg1 are shown in Fig. 2, while Table 9 shows the final PPK parameters estimates of TSL, GRb1 and GRg1.

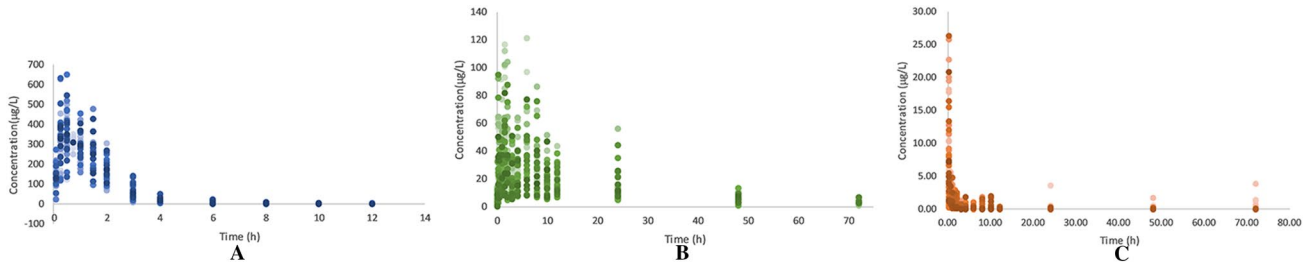

Fig. 2 Mean plasma concentration–time plots of TSL, GRb1, GRg1 after intragastric administration of 1500 mg/kg CDDP to rats. **a** TSL, **b** GRb1, **c** GRg1

Table 9 Summary of the final population pharmacokinetic parameters of TSL, GRb1 and GRg1

Analytes (pharmacokinetic model)	TSL (1-compartment)	GRb1 (1-compartment)	GRg1 (2-compartment)
Population mean parameter			
K_a (1/h)	$3.310\ (\text{week}/14)^{0.915}$	3.203	4.488
V1/F (L)	$6.165\ (\text{WT}/260)^{1.505}$	$57.868\times(\text{WT}/260)^{1.177}$	44.552
V2/F (L)	–	–	653.185
CL1/F (L/h)	$6.842\ (\text{WT}/260)^{0.842}\times\exp(-0.247\times(\text{sex}=0))$	$2.005\times(\text{WT}/260)^{0.675}$	$324.088\times(\text{WT}/260)^{1.494}$
CL2/F (L/h)	–	–	447.976
Interindividual variability			
ω^2_{Ka}	0.215	0.855	0.628
$\omega^2_{\text{V1/F}}$	0.034	0.475	1.999
$\omega^2_{\text{V2/F}}$	–	–	0.283
$\omega^2_{\text{CL1/F}}$	0.043	0.164	0.394
$\omega^2_{\text{CL2/F}}$	–	–	0.288
Residual error	0.318	0.253	0.201

K_a first-order absorption rate constant, *V1/F* apparent volume of distribution of compartment 1, *V2/F* apparent volume of distribution of compartment 2, *CL1/F* apparent total body clearance of compartment 1, *CL2/F* apparent total body clearance of compartment 2, ω^2_{Ka} variance of K_a, $\omega^2_{V1/F}$ variance of V1/F, $\omega^2_{V2/F}$ variance of V2/F, $\omega^2_{CL1/F}$ variance of CL1/F, $\omega^2_{CL2/F}$ variance of CL2/F

For a typical rat (i.e., male; age 14 weeks; weigh 260 g) that received 1500×0.26 mg CDDP once daily, the typical parameters were as follows: for TSL, CL/F was 6.842 L/h, V/F was 6.165 L; For GRb1, CL/F was 2.005 L/h, V/F was 57.868 L; for GRg1, CL/F of compartment 1 was 324.088 L/h, CL/F of compartment 2 was 447.976 L/h, V/F of compartment 1 was 44.552 L, V/F of compartment 1 was 653.185 L. Inter-individual variability (random effects) was estimated for all parameters (i.e., ka, CL/F, and V/F) in the one-compartment model. Relatively large inter-individual variability (ω^2) was observed in V1/F of GRg1($\omega^2_{\text{V1/F}}=1.999$). Goodness-of-fit plots for the final PPK models (Fig. 3) indicated the adequacy of fitting.

Bootstrap validation results (Table 10) were similar to parameters obtained from the original data which indicated that the final model adequately estimated the model parameters. In addition, zero did not include in the 2.5th–97.5th confidence intervals which meant that the results of the estimated parameters were reliable. The VPC showed that most of the observed data of three compounds were within 95% prediction percentiles (Fig. 4). Therefore, these results indicate that the population pharmacokinetic model fitted the observed data and adequately described the population and individual rat plasma concentrations of TSL, GRb1 and GRg1.

4 Discussion

In this study, a simple, rapid and highly sensitive UFLC–MS/MS method for the simultaneous determination of TSL, GRb1 and GRg1 has been successfully developed in rat plasma. We tried to perform the same sample preparation operation which has been reported, but we found that it was difficult to balance the avoidance of material interference with the lower limit of quantitation. We proved that TSL

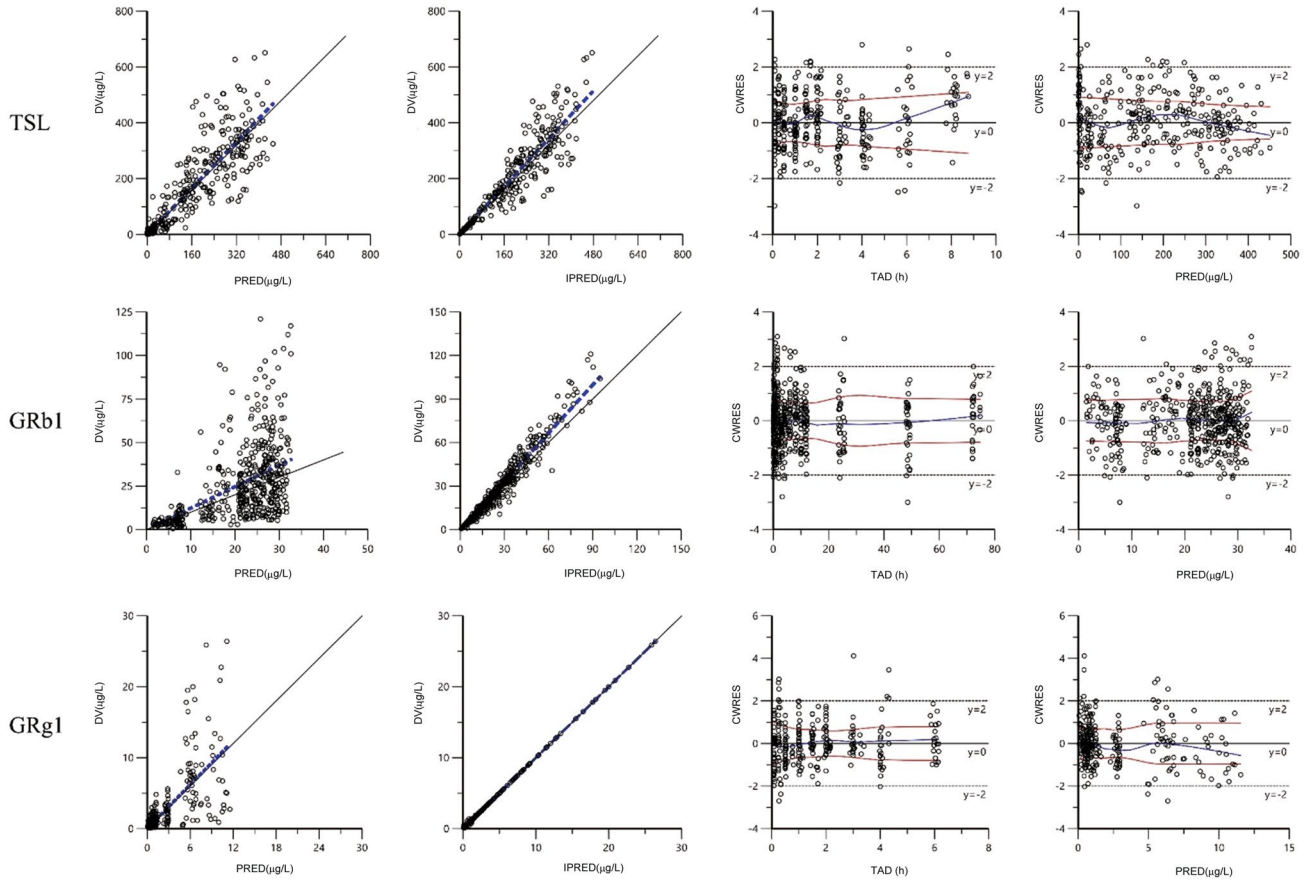

Fig. 3 Goodness-of-fit plots for the final population pharmacokinetic models of TSL, GRb1 and GRg1 in rat plasma after oral administration of CDDP. DV vs. PRED scatterplots, DV vs. IPRED scatterplots, CWRES vs. TAD scatterplots and CWRES vs. PRED scatterplots are displayed from *left* to *right*. The plots showed no remarkable predicted biases and indicate that residual errors are randomly distributed around mean zero. *DV* dependent variable, *PRED* population prediction, *IPRED* individual predicted values, *CWRES* conditional weighted residuals, *TAD* time after dose

had no obvious response when the sample was treated with protein precipitation. When liquid–liquid extraction with ethyl acetate was applied, GRb1 and GRg1 could hardly be detected owing to a very poor recovery. Li et al. [18] reported that the combination of *N*-butanol along with ethyl acetate (1:4, v/v) as well as adding 1% formic acid was chosen as the extraction solution of phenolic acid and saponin components. We found that, when using formic acid, the TSL channel showed other peaks at 2.9 min. Although it did not affect the determination, the LLOQ of TSL was limited. After replacing formic acid with hydrochloric acid, this problem was minimized and the method was more stable. Finally, we used liquid–liquid extraction of three analytes with *N*-butanol-ethyl acetate (1:4, v/v) and 1 M HCl for the sample processing. Proteins supposedly precipitate in acid solution. Adding acid can ensure a higher recovery for both phenolic acid and saponin components, because acid can prevent the binding of analyte to the protein. Meanwhile, acid can also protonate the compounds to their neutral forms, which makes them more soluble in organic solvents than in the ionized salts.

Gradient elution with modified mobile phases (acetonitrile-0.1% formic acid water) was chosen to improve the peak shape of TSL and to improve the signal intensity of ginsenosides. All the analytes were quantified with a high sensitivity within a much shorter time of merely 4.5 min compared with previous similar studies. Good linearity was found in the validated concentration range ($r \geq 0.9924$). The LLOQ were 1.6 ng TSL, 0.5 ng GRb1 and 0.1 ng GRg1/mL plasma, which was three times lower than the method reported by Li et al. [18].

This study was the first to develop the PPK models for the three constituents of CDDP. According to previous studies [18], the GRb1 model was constructed with 72 h data, while the data of GRg1 and TSL were up to 6 and 8 h. Commonly used approaches for handling below the limit of quantification (BLQ) concentrations have been shown to introduce bias in the parameter estimates [24]. In order to reduce the

Table 10 Bootstrap validation results of PPK models of TSL, GRb1 and GRg1

Analytes	Parameters	Unit	Final estimate	Bootstrap validation					
				Mean	SE	CV%	Median	2.50%	97.50%
TSL	tvKa	1/h	3.310	3.339	0.406	12.153	3.294	2.659	4.180
	tvV	L	6.165	6.106	0.357	5.845	6.118	5.383	6.784
	tvCl	L/h	6.842	6.848	0.276	4.025	6.837	6.327	7.394
	dCldsex0		−0.247	−0.250	0.055	−21.903	−0.250	−0.355	−0.143
	dVdweight		1.505	1.520	0.123	8.097	1.511	1.294	1.780
	dCldweight		0.879	0.879	0.081	9.241	0.880	0.714	1.022
	dKadweek		0.915	0.933	0.214	22.942	0.929	0.515	1.387
	stdev0		0.318	0.317	0.023	7.146	0.317	0.275	0.364
GRb1	tvKa	1/h	3.203	3.262	0.393	12.036	3.232	2.607	4.096
	tvV	L	57.868	58.057	3.760	6.476	57.876	51.227	65.878
	tvCl	L/h	2.005	1.980	0.121	6.113	1.974	1.755	2.238
	dVdweight		1.177	1.189	0.169	14.251	1.182	0.877	1.524
	dCldweight		0.675	0.665	0.136	20.394	0.657	0.405	0.945
	stdev0		0.253	0.252	0.023	9.165	0.252	0.209	0.301
GRg1	tvKa	1/h	4.488	4.592	0.713	15.534	4.433	3.647	6.273
	tvV	L	44.552	41.235	12.126	29.407	41.086	18.449	68.571
	tvV2	L	653.185	660.733	108.382	16.403	647.611	482.528	892.266
	tvCl	L/h	324.088	318.186	25.546	8.029	318.013	266.191	367.786
	tvCl2	L/h	447.976	441.037	54.636	12.388	437.599	340.019	554.171
	dCldweight		1.494	1.501	0.184	12.247	1.496	1.170	1.896
	stdev0		0.201	0.200	0.040	20.051	0.201	0.114	0.278

tvKa typical population mean values for Ka, *tvV* typical population mean values for *V*, *tvV2* typical population mean values for *V* of compartment 2, *tvCl* typical population mean values for Cl, *tvCl2* typical population mean values for Cl of compartment 2, *dVdweight* the derivative of the parameter value with respect to weight, *dV* is the increment of volume divided by dweight (the increment of weight), *dCldweight* the derivative of the parameter value with respect to weight, *dCl* the increment of volume divided by dweight, *stdev0* the additive standard deviation

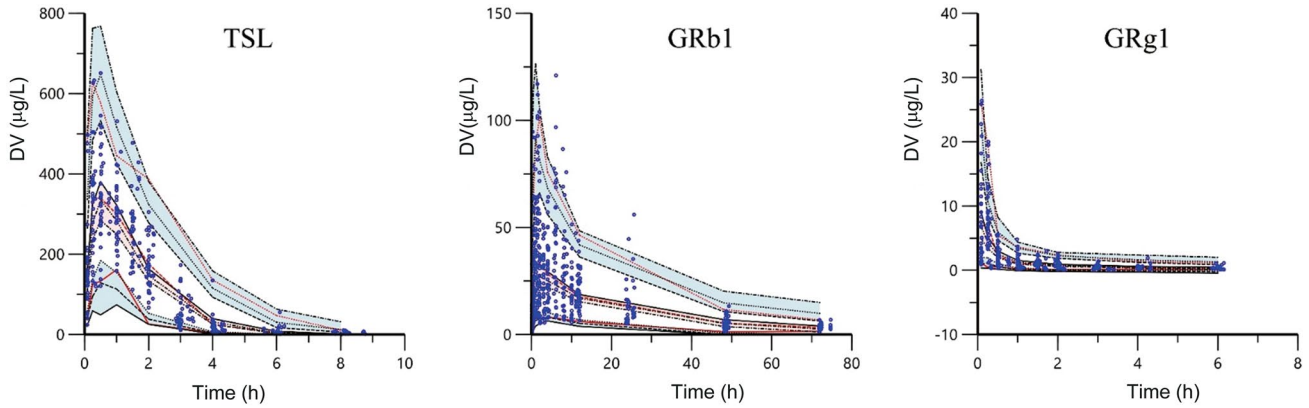

Fig. 4 Visual predictive check for the final PPK models of TSL, GRb1 and GRg1. The *blue circles* indicate the observed concentrations. The *red lines* (from *top* to *bottom*) represent the 95th, median and 5th percentiles of the observed concentrations. The *shaded areas* (from *top* to *bottom*) represent the corresponding 90% prediction interval based on 1000 re-samples

possibility of model misspecification, the BLQ data were not used in this analysis. Table 9 summarizes the final PPK parameters of TSL, GRb1 and GRg1 in rat plasma after oral CDDP.

Three different concentrations (167 mg/kg, 500 mg/kg, 1500 mg/kg) had been chosen as the administration dose of CDDP. However, the content of GRb1 and GRg1 was below the detection limit at the dose of 167 mg/kg and 500 mg/kg.

Additionally, 1500 mg/kg was found as an equivalent dose for rats according to the Phase II&III clinical trials. We also found the $AUC_{0-\infty}$ of TSL (272.11 ± 57.00, 615.9 ± 113.20, 1762.84 ± 438.90 ng/mL h) was proportional to the dose (167 mg/kg, 500 mg/kg, 1500 mg/kg).

Table 6 shows that population pharmacokinetic model of TSL was best described by a one-compartment model with first-order absorption and linear elimination. We chose a multiplicative error model to describe the residual error, and chose exponential models for the inter-individual variability of pharmacokinetic parameters. The population estimate in the base model for K_a, V/F and CL/F were 3.31 h^{-1}, 6.18 L and 6.80 L/h, respectively. Statistically significant covariates consisted of week-Ka, WT-V, gender-CL and WT-CL were added to obtain the final model. The CV% for the pharmacokinetic parameters stayed within the range from 3.95 to 11.34%. The results showed that the clearance rate of TSL is related to gender. Except for the difference in bioavailability, it may also be related to its extensive metabolism in the liver [25], but the mechanisms behind have not yet been clearly understood.

In previous studies, one-compartment was reported for GRb1 pharmacokinetic study in rats [26]. Based on primary drug concentration–time plot, goodness-of-fit plot and the result of the basic model in Table 7, we chose a one-compartment model with first-order absorption and linear elimination as the structural model for GRb1. The inter-individual variability was calculated by exponential models for the three pharmacokinetic parameters, and residual error by a multiplicative model. The final model contained WT-V/F and WT-CL/F, where the CV% values for all the estimated parameters were below 16.23%.

Disposition of GRg1 in rat plasma was established by a two-compartment model and clearance was adequately described with linear elimination, as shown in Table 8. The random effects included residual error estimated by an additive model with the low concentration of GRg1 in vivo. Inter-individual variability was estimated by exponential models. The introduction of WT-CL decreased AIC from 881.7 to 834.7. The CV% values of the estimates were acceptable, with a range of 8.03–42.43%. Saponins are mainly metabolized by intestinal flora, and the metabolites absorbed into the body are less metabolized by the liver. Most saponins play their pharmacological role directly by secondary glycosides or aglycones [27]. In this study, we did not observe a significant relationship between ginsenoside metabolism and gender, which was consistent with previous research.

As can be seen from Fig. 3, there were still deviations between PRED and DV in the final model of ginsenosides. Quantitative effects of intestinal flora differences on drug metabolism need to be further studied. Figure 4 shows good association between the observed and predicted concentrations. Although it has only been a preclinical study at present, the influence of gender and age and other factors on drug metabolism also has reference value for CMM clinical application.

There are still some deficiencies in the present study and further research is needed. We did not include experiments to compare the sparse sampling approach with traditional dense sampling, since sparse sampling is widely accepted in small animal pharmacokinetic space and the pharmacokinetic profiles of TSL, GRb1 and GRg1 are not thought to be variable. Secondly, the pharmacological mechanism of each compound has not been thoroughly studied. To a certain extent, this may restrict the PPK study of the three compounds. From further study, it seems necessary to compare the pharmacokinetic of the three compounds after administering CDDP and the pharmacokinetic after administering each compound alone. Thirdly, the PPK model was not confirmed in a different cohort. In addition to bootstrap validation and VPC, external validation studies are also needed to confirm the predictability of the PPK models.

5 Conclusion

Simultaneous determination methods of TSL, GRb1 and GRg1 in rat plasma were established by using UFLC–MS/MS system. The specificity, accuracy, precision and matrix effects of the methods met the requirements of biological sample determination. On this basis, we first constructed the population pharmacokinetic models of TSL, GRb1 and GRg1 in rats after oral CDDP, and the relationship between pharmacokinetic parameters and physiological information of rats was also clarified. Compared with previous CMM pharmacokinetic studies, this study took advantage of sparse sampling and quantitative prediction of variation, which can more effectively explain drug application information. As a preliminary exploration toward the clinical population pharmacokinetic research, this study provides a reference for the population pharmacokinetic study of traditional Chinese medicine.

Compliance with Ethical Sstandards

Funding The experiment is supported by Tianjin Science & Technology Plan Project [16PTSYJC00270]; Tianjin Science & Technology Plan Project [18YFZCSY00110].

Conflict of Interest There is no conflict of interest in this paper.

Ethics Approval All animals were handled according to the guidelines of the Tasly Animal Research Committee, and the experimental protocols were approved by the Animal Ethics Committee of Tasly Institute (TSL-IACUC-2013–015). All animal procedures conform to the NIH guidelines on the protection of animals.

References

1. Luo J, Song W, Yang G, Xu H, Chen K. Compound Danshen (Salvia miltiorrhiza) dripping pill for coronary heart disease: an overview of systematic reviews. Am J Chin Med. 2015;43(1):25–43. https://doi.org/10.1142/S0192415X15500020.
2. Zhang L, Zheng J, Li H, Meng Y. Inhibitory effects of cardiotonic pills on platelet function in dogs fed a high-fat diet. Blood Coagul Fibrinolysis. 2006;17(4):259–64. https://doi.org/10.1097/01.mbc.0000224844.33216.91.
3. Guo J, Yong Y, Aa J, Cao B, Sun R, Yu X, et al. Compound danshen dripping pills modulate the perturbed energy metabolism in a rat model of acute myocardial ischemia. Sci Rep. 2016;6:37919. https://doi.org/10.1038/srep37919.
4. Zhao N, Liu Y, Wang F, Hu B, Sun K, Chang X, et al. Cardiotonic pills, a compound Chinese medicine, protects ischemia-reperfusion-induced microcirculatory disturbance and myocardial damage in rats. Am J Physiol Heart Circ Physiol. 2010;298(4):H1166–H1176176. https://doi.org/10.1152/ajpheart.01186.2009.
5. Lam FF, Yeung JH, Chan KM, Or PM. Relaxant effects of danshen aqueous extract and its constituent Danshensu on rat coronary artery are mediated by inhibition of calcium channels. Vascul Pharmacol. 2007;46(4):271–7. https://doi.org/10.1016/j.vph.2006.10.011.
6. Chan K, Chui S, Wong D, Ha W, Chan C, Wong R. Protective effects of Danshensu from the aqueous extract of Salvia miltiorrhiza (Danshen) against homocysteine-induced endothelial dysfunction. Life Sci. 2004;75(26):3157–71. https://doi.org/10.1016/j.lfs.2004.06.010.
7. Yang B, Cheung K, Zhou X, Xie R, Cheng P, Wu S, et al. Amelioration of acute myocardial infarction by saponins from flower buds of Panax notoginseng via pro-angiogenesis and anti-apoptosis. J Ethnopharmacol. 2016;181:50–8. https://doi.org/10.1016/j.jep.2016.01.022.
8. Zhou Z, Wang J, Song Y, He Y, Zhang C, Liu C, et al. Panax notoginseng saponins attenuate cardiomyocyte apoptosis through mitochondrial pathway in natural aging rats. Phytother Res. 2018;32(2):243–50. https://doi.org/10.1002/ptr.5961.
9. Huo M, Wang Z, Wu D, Zhang Y, Qiao Y. Using coexpression protein interaction network analysis to identify mechanisms of Danshensu affecting patients with coronary heart disease. Int J Mol Sci. 2017. https://doi.org/10.3390/ijms18061298.
10. Fan G, Yu J, Asare PF, Wang L, Zhang H, Zhang B, et al. Danshensu alleviates cardiac ischaemia/reperfusion injury by inhibiting autophagy and apoptosis via activation of mTOR signalling. J Cell Mol Med. 2016;20(10):1908–19. https://doi.org/10.1111/jcmm.12883.
11. Fang X, Liu Y, Lu J, Hong H, Yuan J, Zhang Y, et al. Protocatechuic aldehyde protects against isoproterenol-induced cardiac hypertrophy via inhibition of the JAK2/STAT3 signaling pathway. N S Arch Pharmacol. 2018;391(12):1373–85. https://doi.org/10.1007/s00210-018-1556-7.
12. Zheng Q, Bao X, Zhu P, Tong Q, Zheng G, Wang Y. Ginsenoside Rb1 for myocardial ischemia/reperfusion injury: preclinical evidence and possible mechanisms. Oxid Med Cell Longev. 2017;2017:6313625. https://doi.org/10.1155/2017/6313625.
13. Cui Y, Pan C, Yan L, Li L, Hu B, Chang X, et al. Ginsenoside Rb1 protects against ischemia/reperfusion-induced myocardial injury via energy metabolism regulation mediated by RhoA signaling pathway. Sci Rep. 2017;7:44579. https://doi.org/10.1038/srep44579.
14. Fan J, Liu D, He C, Li X, He F. Inhibiting adhesion events by Panax notoginseng saponins and ginsenoside Rb1 protecting arteries via activation of Nrf2 and suppression of p38 - VCAM-1 signal pathway. J Ethnopharmacol. 2016;192:423–30. https://doi.org/10.1016/j.jep.2016.09.022.
15. Li L, Pan C, Yan L, Cui Y, Liu Y, Mu H, et al. Ginsenoside Rg1 ameliorates rat myocardial ischemia-reperfusion injury by modulating energy metabolism pathways. Front Physiol. 2018;9:78. https://doi.org/10.3389/fphys.2018.00078.
16. Li Q, Xiang Y, Chen Y, Tang Y, Zhang Y. Ginsenoside Rg1 protects cardiomyocytes against hypoxia/reoxygenation injury via activation of Nrf2/HO-1 signaling and inhibition of JNK. Cell Physiol Biochem. 2017;44(1):21–37. https://doi.org/10.1159/000484578.
17. Lu T, Yang J, Gao X, Chen P, Du F, Sun Y, et al. Plasma and urinary tanshinol from *Salvia miltiorrhiza* (Danshen) can be used as pharmacokinetic markers for cardiotonic pills, a cardiovascular herbal medicine. Drug Metab Dispos. 2008;36(8):1578–86. https://doi.org/10.1124/dmd.108.021592.
18. Li T, Chu Y, Yan K, Li S, Wang X, Wang Y, et al. Simultaneous determination of tanshinol, protocatechuic aldehyde, protocatechuic acid, notoginsenoside R1, ginsenoside Rg1 and Rb1 in rat plasma by LC-MS/MS and its application. Biomed Chromatogr. 2017. https://doi.org/10.1002/bmc.3889.
19. Li W, Zhou H, Chu Y, Wang X, Luo R, Yang L, et al. Simultaneous determination and pharmacokinetics of danshensu, protocatechuic aldehyde, 4-hydroxy-3-methyloxyphenyl lactic acid and protocatechuic acid in human plasma by LC-MS/MS after oral administration of Compound Danshen dripping pills. J Pharm Biomed Anal. 2017;145:860–4. https://doi.org/10.1016/j.jpba.2017.06.014.
20. Wang X, Li W, Ma X, Yan K, Chu Y, Han M, et al. Identification of a major metabolite of danshensu in rat urine and simultaneous determination of danshensu and its metabolite in plasma: application to a pharmacokinetic study in rats. Drug Test Anal. 2015;7(8):727–36. https://doi.org/10.1002/dta.1750.
21. Pei W, Zhao X, Zhu Z, Lin C, Zhao W, Zheng X. Study of the determination and pharmacokinetics of Compound Danshen Dripping Pills in human serum by column switching liquid chromatography electrospray ion trap mass spectrometry. J Chromatogr B 2004;809(2):237–42. https://doi.org/10.1016/j.jchromb.2004.06.028.
22. Xu Q, Fang X, Chen D. Pharmacokinetics and bioavailability of ginsenoside Rb1 and Rg1 from Panax notoginseng in rats. J Ethnopharmacol. 2003;84(2–3):187–92.
23. Williams PJ, Ette EI. The role of population pharmacokinetics in drug development in light of the Food and Drug Administration's 'Guidance for Industry: population pharmacokinetics'. Clin Pharmacokinet. 2000;39(6):385–95. https://doi.org/10.2165/00003088-200039060-00001.
24. Byon W, Smith MK, Chan P, Tortorici MA, Riley S, Dai H, et al. Establishing best practices and guidance in population modeling: an experience with an internal population pharmacokinetic analysis guidance. CPT Pharmacometrics Syst Pharmacol. 2013;2:e51. https://doi.org/10.1038/psp.2013.26.
25. Li S, Wang X, Li W, Chu Y, Guo J, Ma X, et al. Characterization of metabolites in rat after administration of Danshensu by liquid chromatography-tandem mass spectrometry. Lat Am J Pharm. 2013;32(4):582–6.
26. Munekage M, Ichikawa K, Kitagawa H, Ishihara K, Uehara H, Watanabe J, et al. Population pharmacokinetic analysis of daikenchuto, a traditional Japanese medicine (Kampo) in Japanese and US health volunteers. Drug Metab Dispos. 2013;41(6):1256–63. https://doi.org/10.1124/dmd.112.050112.
27. Odani T, Tanizawa H, Takino Y. Studies on the absorption, distribution, excretion and metabolism of ginseng saponins. IV. Decomposition of ginsenoside-Rg1 and -Rb1 in the digestive tract of rats. Chem Pharm Bull (Tokyo). 1983;31(10):3691–7.